LINC00908 promotes malignant progression and glycolysis in lung adenocarcinoma via interactions with DDX54 and RFX2

Xuhui Yang
The Fifth Medical Center, Chinese PLA General Hospital and Chinese PLA Medical School
Jiahua Zhao
The Sixth Medical Center, Chinese PLA General Hospital and Chinese PLA Medical School
Yang Zhang
The Second Medical Center, Chinese PLA General Hospital
Lin Zhang
986th Hospital Affilliated to Air Force Medical University
Lijie Wang
The Fifth Medical Center, Chinese PLA General Hospital and Chinese PLA Medical School
Fan Zhang
The Fifth Medical Center, Chinese PLA General Hospital and Chinese PLA Medical School
Xiao Han
The Fifth Medical Center, Chinese PLA General Hospital and Chinese PLA Medical School
Haitao Tao
The Fifth Medical Center, Chinese PLA General Hospital and Chinese PLA Medical School
Chenxi Li
The Fifth Medical Center, Chinese PLA General Hospital and Chinese PLA Medical School
Xiang Zhu
Army No.82 Group Military Hospital
Yi Hu (huyi301zlxb@sina.com)
the Fifth Medical Center, Chinese PLA General Hospital

Article

Keywords:

Posted Date: January 25th, 2023

DOI: https://doi.org/10.21203/rs.3.rs-2405866/v1

Abstract

Lung adenocarcinoma (LUAD) is one of the leading causes of cancer-related death worldwide. We identified a specific LncRNA, LINC00908, was downregulated in LUAD tissues and associated with good outcome. LINC00908 inhibited glycolysis by regulating the expression of the DEAD-box54 (DDX54), which was screened by a nine-gene risk signature related to glycolysis and positively correlated with parts of glycolysis-related genes. DDX54 was also experimental verified that regulate nine key glycolytic enzymes, thereby affecting the level of glycolysis in LUAD. Further, the expression of LINC00908 in LUAD tumorigenesis was modulated by a transcription factor, RFX2. The RFX2/LINC00908/DDX54 axis regulated LUAD tumor growth, migration, invasion, cell apoptosis and glycolysis both in vitro and in vivo. These results demonstrated that this axis might be a novel mediator in LUAD progress. We might offer a novel therapeutic target for more precise diagnosis and treatment of LUAD.

Introduction

Lung cancer is the leading reason of tumor-associated death worldwide. The incidence rate of lung cancer increased 4.5% every year [1, 2]. LUAD is the important histological type of lung cancer. In recent decades, targeted therapy and oncogene identification have made great strides [3], however, a large proportion of LUAD still lack effective targeted therapy options.

Reprogramming the energy metabolism is characterized by the "Warburg effect," one of the most important emerging markers of cancer [4, 5]. It is widely characterized that high levels of glycolysis occur regardless of the existence of oxygen. Glycolysis process gives access to changes of glucose uptake, lactic acid production and ATP production to promote tumor growth and progressions [6]. Moreover, the activities of glycolytic enzymes play key roles in the growth and progression of cancer. Therefore, glycolysis is a complex, multi-step and long-term process in the development of most cancer types including LUAD [7].

Over the past decades, it is generally accepted that noncoding RNAs (ncRNAs) play a crucial role in the regulation of gene expression, including the phenotype of normal or tumor cells [8]. Long noncoding RNAs (LncRNAs) are normally considered as genomic transcripts with a length of more than 200 nucleotides. Due to the deficiency of open reading structure of the necessary length, LncRNAs cannot encode proteins. However, plenty of existing studies have confirmed that LncRNAs are involved in the oncogenesis and progression of tumors so as to be effective cancer biological molecular biomarkers and potential therapeutic targets [9]. LncRNAs are found to have profound impacts on diverse downstream targets. Importantly, LncRNAs could act as competitive endogenous RNAs (ceRNAs) to upregulate mRNAs expression through adsorbing microRNAs. For example, LINC-PINT regulates miR-767-5p biogenesis in thyroid cancer [10]. Besides, tumor oncogenesis can be regulated by LncRNAs through binding to RNA binding protein (RBP), so as to maintain mRNA's stability. LBX2-AS1 positively regulated LBX2 mRNA stability via FUS.

DEAD box (DDX) proteins belong to the largest subfamily of RNA helicase SF2, which unfold RNA double strand and participate in multiple processes of RNA metabolism, including RNA cutting, editing, output and degradation, as well as the conduct of ribosome generation, transcription and translation [11]. At present, more than 50 DDX family members have been found and studied in cancer, such as DDX3, DDX5 [12–14] etc. Therefore, DDX memberships might be potential targets for tumor diagnosis, prognosis evaluation and drug treatment. DDX54 has been proved to be a hormone dependent interacting protein of estrogen receptors (ERs) and CAR-binding protein [15, 16]. In addition, DDX54 involves in DNA damage repair, promoting the growth of gastric cancer cells and the formation of myelin sheath of nerve cells [17]. However, the precise function and mechanisms of DDX54 in LUAD have not been established.

In our study, LINC00908 was first proved to be negatively correlated with DDX54 and predicted a good clinical prognosis in LUAD. Mechanistically, LINC00908 inhibits the expression of glycolysis related genes by downregulating the expression of DDX54. In addition, the expression of LINC00908 is mainly activated by the transcription factor, RFX2. The results show that RFX2/LINC00908/DDX54 axis regulates glycolysis, tumor growth and lung metastasis of LUAD in vitro and in vivo. Our study established RFX2/LINC00908/DDX54 as a new key axis to regulate the growth and progress of LUAD.

Materials And Methods

Human tumor tissues and Cell lines

Normal lung cell line (16HBE) and LUAD cell lines (A549, PG49, H1299, Calu3) used in this study were all incubated in dulbecco's modified eagle medium (GIBCO, USA) blended with fetal bovine serum (10%), penicillin (100 IU/mL) and streptomycin (100 mg/mL) at 37°C with 5% CO_2.

130 samples were acquired from LUAD patients who underwent surgery between March to September 2019 at Chinese PLA General Hospital. The Ethics Committee of Chinese PLA General Hospital supervised all experimental processes.

Analysis of TCGA-LUAD dataset

The Cancer Genome Atlas (https://portal.gdc.cancer.gov/repository) was used to download RNA-Sequencing and corresponding clinical information of TCGA-LUAD. Analysis of differentially expressed lncRNAs/mRNAs ($|\log2FC| > 1$ and P-value < 0.05) using limma package in R. The correlation between different lncRNAs/mRNAs was analyzed by the Spearman algorithm. We utilized KMplotter to explore lncRNA or mRNA related to the prognosis of LUAD patients. The gene enrichment analysis (GSEA) was manipulated to find possible mechanism of tumorigenesis in LUAD.

Quantitative real-time PCR (qRT-PCR)

RNA was obtained from human tumor tissues or cells by using Trizol reagent as the manufacturer's instructions. RNA was transcribed into cDNA and qPCR was performed three times. The comparative Ct value represents the relative expression. Specific primer sequences are listed in Table S1.

Western blot

After being harvested, cells and tissues were broken in RIPA lysis buffer. The mixture proteins were separated on SDS-PAGE gels. The polyvinylidene fluoride (PVDF) membrane was used to transfer cell lysates. The primary antibodies and secondary antibodies were then employed sequentially. The primary antibodies as follows: anti-DDX54 (26894-1-AP, Proteintech; 1:1,000 dilution), anti-RFX2 (ab79241, Abcam; 1:500 dilution), anti-β-actin (sc-47778, Santa Cruz Biotechnology; 1:1,000 dilution), anti-SLC2A1 (21829-1-AP, Proteintech; 1:500 dilution), anti-HK2 (2867S, Cell Signaling Technology; 1:500 dilution), anti-GPI (sc-33777, Santa Cruz Biotechnology; 1:500 dilution), anti-PFKL (sc-292523, Santa Cruz Biotechnology; 1:500 dilution), anti-ALDOA (11217-1-AP, Proteintech; 1:1,000 dilution), anti-GAPDH (G9295, Sigma-Aldrich; 1:1,000 dilution), anti-PGK1 (17811-1-AP, Proteintech; 1:1,000 dilution), anti-PGAM1 (16126-1-AP, Proteintech; 1:1,000 dilution), anti-ENO1 (sc-15343, Santa Cruz Biotechnology; 1:500 dilution), anti-PKM (sc-365684, Santa Cruz Biotechnology; 1:500 dilution), anti-LDHA (19987-1-AP, Proteintech; 1:1,000 dilution).

Cell proliferation, colony-formation, and apoptosis assays

CCK-8 was used to detect and compare the proliferation ability of cells following the instructions. Cells (3×10^3/well) were cultured in a 3.5 cm plate for 2 weeks. After rinsing the cells twice with PBS, fix the cells with 4% formaldehyde for 30 minutes. Rinsing twice with PBS again, and then staining cells with 0.1% crystal violet solution for 30 min. Colonies larger than 1.5mm in diameter were counted and compared. Cells were dissociated to detect apoptosis rates. Apoptosis cells were stained with Annexin V Apoptosis Detection kit and detected with flow cytometry.

Cell migration and invasion assays

Filled the plate with cells and drew a straight line on the cells with 200 μL pipette tips. Cells were cultured for 24 h. The wound edges were photographed and calculated. Cell invasion chambers were applied to detect cell invasion as the manufacturer's protocol. The detected cells were cultured into the upper chamber by medium without serum. After 24h, 4% paraformaldehyde was used to fix cells adhering on the surface of the chambers. Rinsed twice with PBS again, stained cells with 0.5% crystal violet, and photographed with a microscope.

Extracellular Acidification Rate and Oxygen Consumption Rate assay

The Seahorse XFe96 Extracellular Flux Analyzer was used to detect Extracellular Acidification Rate (ECAR) and cellular Oxygen Consumption Rate (OCR) as the manufacturer’s protocols. The indicated cells were resuspended and counted. 10, 000 cells were transferred into Seahorse XF96 cell culture microtiter plate. Both for ECAR or OCR detection, the baselines were detected first. Glucose, oligomycin and 2-deoxyglucose were added in proper time and ordered for ECAR. Oligomycin, FCCP, and Rote/AA were added in proper time and ordered for OCR. ECAR values are shown as mpH/min and OCR values are shown as pmols/min.

Chromatin immunoprecipitation (ChIP) assay

For ChIP assays, cells were fixed with formaldehyde to form DNA-protein mixture for 10 min. The fixation reaction was stopped when the glycine was added. The cell lysates were subjected to sonication treatment and immunoprecipitated with specific antibodies. DNA was extracted and purified from the immunoprecipitated complex and analyzed by PCR.

Luciferase reporter assay

The promoter of LINC00908 and different segments were constructed into pGL3.0-basic vector respectively. Cells were co-transfected with luciferase reporters. Luciferase activities were measured after 24 h in term of the manufacturer's protocol.

Hematoxylin-eosin and IHC assay

Paraffin-embedded tissues were sectioned to 4 mm thickness. The samples were successively washed and incubated with indicated primary antibodies after incubating with antigen retrieval solution. Washing and incubating corresponding secondary antibodies, visualized after 3,3-diaminobenzidine (DAB) and hematoxylin staining.

Tumor growth and metastasis analysis in vivo

To assess cell proliferation in vivo, 1×10^7 A549 cells were injected into the axillary fossae of nude mice. Overall survival and tumor size were evaluated at the indicated times. Recorded The time of mice being sacrificed. The Ethics Committee of Chinese PLA General Hospital supervised all of the animal experiments.

Statistical analysis

All data were shown as averages from the results of at least three independent experiments. GraphPad 8.0 and SPSS 22.0 were used for statistical analysis of all experimental data. The difference between two groups was analyzed by two-tailed Student's test, and three groups or more groups were tested by ANOVA. A p value of less than 0.05 was considered statistically significant. All experiments were repeated at least three times.

Results

Screening of LncRNAs and characterization of LINC00908 in LUAD.

To explore new effective LncRNAs regulating glycolysis in LUAD, we analyzed the data related to LUAD according to the screening strategy (Fig. 1A). The differentially expressed LncRNAs in normal and cancer tissues were achieved using data from TCGA database. As shown in Fig. 1B, there were 1843 LncRNAs exhibited differentially expression, including 992 upregulated and 851 downregulated LncRNAs in paired samples. In addition, 1906 differentially expressed LncRNAs were screened in unpaired samples involving 883 upregulated and 1023 downregulated LncRNAs (Figure S1). To sum up, there were 1491 overlapped

LncRNAs comprising 790 upregulated and 701 downregulated LncRNAs (Fig. 1C). Next, we analyzed these differentially expressed LncRNAs related to survivable prognosis by independent prognostic analysis. The overall prognosis was correlated with 8 upregulated, including LINC00908, and 5 downregulated LncRNAs (Fig. 1D). Subsequently, we decided to explore the correlation between the prognosis-associated LncRNAs and a nine-gene risk score associated with glycolysis. Interestingly, LINC00908 had the greatest correlation coefficient with risk score among these 13 LncRNAs (Fig. 1E), indicating its possible important role in LUAD. Moreover, the expression of LINC00908 in normal tissues was higher than that in tumor tissues (Figs. 1F, G). Further analysis found that LINC00908 showed a good clinical outcome in LUAD (Fig. 1H). Additionally, we analyzed LUAD RNA-seq data for gene set enrichment analysis (GSEA). Consistently, LINC00908 was negatively correlated with poor survival of lung cancer (Fig. 1I). To further explore specific functions of LINC00908 in LUAD, RNA levels were determined in 10 pairs of LUAD tissues and their matched adjacent normal tissues by qRT-PCR. The results similarly demonstrated that LINC00908 expressions in cancer tissues were significantly lower than that in normal tissues (Fig. 1J). Notably, LINC00908 expressions in tumor cells were lower than that in normal lung epithelial cells, remarkably in A549 and H1299 cells (Fig. 1K).

DDX54, a negative prognostic factor for LUAD, is regulated by LINC00908.

The mechanisms by which LINC00908 regulated glycolysis in LUAD were further explored. First, LUAD samples were divided into high and low risk score sets from TCGA employing the above-mentioned nine-gene risk signature model. There were 1 upregulated and 1837 downregulated differential expressed genes in our screen (Fig. 2A). Second, 25 target genes that might be regulated by LINC00908 were predicted based on the Starbase database. Third, an intersection of both the 25 target genes and 1838 differential expressed genes were conducted. Finally, we obtained 3 potential genes, DDX54, IGF2BP3 and TAF15, triggered by LINC00908. (Fig. 2B). Excitingly, the highest correlation was observed between DDX54 and LINC00908 (Fig. 2C, Figure S2). We thus gave priority to the possible regulatory relationship between LINC00908 and DDX54. In 10 LUAD and adjacent tissues, LUAD tissues contained higher levels of DDX54 mRNA and protein than adjacent tissues (Fig. 2D). Similarly, DDX54 was significantly increased in both paired and unpaired analysis based on TCGA database (Fig. 2E). Furthermore, high DDX54 expression levels resulted in a poor OS in LUAD (Fig. 2F). In addition, the pivotal results were that knockdown of LINC00908 significantly fueled DDX54 expressions both in A549 and H1299 cells (Fig. 2G). In total, the intrinsic mechanisms of DDX54 and LINC00908 in LUAD deserved to be estimated.

LINC00908 inhibition facilitated LUAD tumorigenesis through mediating DDX54 in vitro.

Next, we detected the roles of LINC00908 and DDX54 on the growth, apoptosis, migration and invasion in independent LUAD cells. LINC00908 overexpression decreased the protein levels of DDX54 in both A549 and H1299 cells. Remarkably, this impairing effect can be reversed by DDX54 overexpression in the cells transfected LINC00908 (Fig. 3A). Next, CCK8, apoptosis, wound healing, colony assay and transwell assays were conducted. As shown, LINC00908 overexpression decreased the proliferation, migration, invasion in both LUAD cells. Moreover, apoptosis assays indicated that overexpression of LINC00908

could reduce cell apoptosis. Further, cotransfected DDX54 and LINC00908 abolished these effects generated by LINC00908 overexpression (Figs. 3B-E).

On the other hand, we explored whether the effects of LINC00908 knockdown depend on DDX54 in both LUAD cells. As expected, LINC00908 knockdown demonstrably upregulated the ability of proliferation, migration, invasion and downregulated apoptosis. DDX54 consistently restrained these effects of LINC00908 (Figs. 4A-E). Collectively, these data demonstrated that LINC00908 dampens the growth, migration and invasion through DDX54 in LUAD cells. Overexpression of LINC00908 could restrain LUAD progression, and this role of tumor suppressor mainly depended on DDX54 expression in LUAD cells.

DDX54 knockdown downregulates glycolysis in LUAD cells.

We also conducted GSVA analysis to detect the relationship between DDX54 and glycolysis-related pathways. There were 6 pathways implicated in glycolysis, involving KEGG_GLYCOLYSIS_GLUCONEOGENESIS, REACTOME_GLYCOLYSIS, WINTER_HYPOXIA_UP, MOOTHA_GLYCOLYSIS, WINTER_HYPOXIA_DN, GROSS_HYPOXIA_VIA_HIF1A_UP, QI_HYPOXIA_TARGETS_OF_HIF1A_AND_FOXA2 (Figs. 5A-C, Figure S3).

Additionally, we interrogated the possible correlations between DDX54 and 12 glycolysis-related genes according to the database from TCGA. Strong positive correlations were detected between DDX54 and 11 genes (SLC2A1, HK2, GPI, PFKL, ALDOA, GAPDH, PGK1, PGAM1, ENO1, PKM, and LDHA) (Figs. 5D, E). We further found that DDX54 knockdown downregulated the mRNA and protein expressions of SLC2A1, GPI, PFKL, ALDOA, PGK1, PGAM1, ENO1, PKM in both LUAD cells. Excitingly, these outcomes were reversed via reexpression of DDX54 in DDX54 knockdown cells (Figs. 5F, G), which provided further evidence of DDX54 in glycolysis. Moreover, there was a decrease in ECAR and an increase in OCR with DDX54 knockdown, indicating lower glycolytic flux and higher mitochondrial respiration. Once more, DDX54 reexpression reversed these effects (Figs. 5H, I). Besides, glucose uptake, lactate production, ATP generation, and pyruvate were tested to evaluate the glycolysis level. Corresponding with expected, DDX54 knockdown decreased glucose uptake, lactate production, ATP generation, and pyruvate, while DDX54 reexpression reversed these effects (Figs. 5J, K). To sum up, these data suggested that DDX54 knockdown downregulates glycolysis in both A549 and H1299 cells.

LINC00908 downregulates glycolysis through DDX54 in vitro.

Since we proved the regulatory relationship between LINC00908 and DDX54, we next explored whether LINC00908 plays an important role in regulating glycolysis. GSVA analysis revealed that LINC00908 was negative correlated with KEGG_GLYCOLYSIS_GLUCONEOGENESIS, REACTOME_GLYCOLYSIS, WINTER_HYPOXIA_UP, GROSS_HYPOXIA_VIA_HIF1A_UP, REACTOME_REGULATION_OF_GLYCOLYSIS_BY_FRUCTOSE_2_6_BISPHOSPHATE_METABOLISM (Figs. 6A-C, Figure S4). In vitro, LINC00908 knockdown upregulated the mRNA and protein levels of DDX54, SLC2A1, GPI, PFKL, ALDOA, PGK1, PGAM1, ENO1, PKM. DDX54 knockdown abolished these effects in both cells (Figs. 6D, E, I, K). Moreover, the results of glucose uptake, lactate production, ATP

generation, pyruvate, ECAR and OCR also confirmed the effects of LINC00908 inhibiting glycolysis via DDX54 (Figs. 6F, G, H, J, L, M).

RFX2 was screened as one of the transcript factors for LINC00908.

We predicted 383 transcription factors which may bind to the promoter region of LINC00908 using the bioinformatics database. These predicted transcription factors were then overlapped with the results of DEGs from the analysis results based on TCGA database. Finally, we obtained 40 candidate transcription factors (Fig. 7A), of which 28 were associated to positive prognostic impact in LUAD. One of these, RFX2, is of particular interest. Because further analyses showed that there were significant correlations between RFX2 and LINC00908 (Figs. 7B-D). Immunoblot analysis and qPCR showed that Based on the important role of RFX2 in LUAD, we then detected the mRNA and protein expressions of RFX2 in 10 pairs of tumor and adjacent tissues. The results demonstrated that RFX2 expression was significantly lower in tumor tissues than that in adjacent tissues (Fig. 7E). Besides, similar results were confirmed in paired or unpaired LUAD samples from TCGA database (Fig. 7F). Thus, it is of importance to further investigate the specific association between RFX2 and LINC00908. We predicted the expected binding sites by a bioinformatics method (http://jaspar.genereg.net/). We then found that RFX2 overexpression increased the LINC00908 promoter reporter activity containing the putative RFX2-binding site, whereas the mutated binding site had little effect on RFX2 activation of the LINC00908 promoter (Fig. 7G). Consistent with this, chromatin immunoprecipitation (ChIP) assay showed that RFX2 was proved to bind to the LINC00908 promoter, not upstream (Fig. 7H). These results suggested that RFX2 might be one of the critical transcription factors for LINC00908.

RFX2 suppresses proliferation, apoptosis, migration, invasion and glycolysis by regulating LINC00908 in LUAD cells.

Subsequently, we validated the possible association between RFX2 and LINC00908 in regulation of LUAD progressions. The results showed that RFX2 overexpression inhibited LUAD cell growth, while LINC00908 knockdown lead to RFX2 inactivation in regulating cell proliferation (Figs. 8A-B). We further explored whether RFX2 inhibits cell apoptosis, migration, and invasion via LINC00908. As expected, RFX2 overexpression inhibited LUAD cell apoptosis, migration, and invasion. LINC00908 knockdown greatly dampened these effects of RFX2 overexpression (Figs. 8C-G).

We also detected the functions of RFX2 on glycolysis in LUAD. RFX2 overexpression suppressed glycolytic genes, including SLC2A1, GPI, PFKL, ALDOA, GAPDH, PGAM1, ENO1, and PKM. had reduced mRNA and protein expression levels of DDX54 and Moreover, these functions of RFX2 were abolished by LINC00908 knockdown (Figs. 9A-D). Further studies also revealed that RFX2 dampened glucose uptake, lactate production, ATP generation, and pyruvate ratio. This reduction could also be reversed by LINC00908 knockdown (Figs. 9E, F). Corresponding with the above results, RFX2 displayed decreased ECAR and increased OCR, which were abolished by LINC00908 knockdown (Figs. 9G-J). Taken together, these data showed that RFX2 suppresses LUAD cell growth, apoptosis, migration, invasion, and glycolysis largely dependent on LINC00908.

RFX2/LINC00908/DDX54 axis has a tumor-promoting effect in vivo.

We next aimed to investigate the phenotype of the RFX2/LINC00908/DDX54 pathway in vivo. First, Injecting BALB/c mice with A549 cells carrying the indicated constructs was performed subcutaneously. We detected that LINC00908 knockdown significantly elevated LUAD tumor growth, whereas knockdown of DDX54 blocked tumor growth. Furthermore, DDX54 knockdown evidently elucidated the regulation by LINC00908 in the tumor growth of xenografts (Figs. 10A-D). Next, we examined the important roles of RFX2 and LINC00908 in the regulation of LUAD tumor growth. As shown in Figs. 10E-G, RFX2 overexpression significantly decreased LUAD tumor growth, while this effect was dramatically attenuated when LINC00908 was knocked down. These data suggesting the key role of RFX2/LINC00908/DDX54 axis in vivo.

Clinical Relevance of LINC00908, DDX54 and RFX2 in the LUAD patients.

We performed immunohistochemical (IHC) staining to assess DDX54 expression and FISH assays to examine LINC00908 expression in 130 human LUAD samples. Positive correlation was found between LINC00908 expression and RFX2 expression, but negative correlation with DDX54 expression (Figs. 11A, B). The potential regulatory pathway is shown in Fig. 8C. Overall, these results indicated that RFX2/LINC00908/DDX54 axis is likely to play important pathological roles in LUAD.

Discussion

Enhanced glycolysis was proved to be a metabolic characteristic of numerous cancers, which is affected by several key factors, including hypoxia, ubiquitination, metabolic stress [18–20] etc. In recent years, LncRNAs have been increasingly reported to function as promoting or suppressing roles in glycolytic pathway [21, 22]. For example, in LUAD, LINC00857 regulated the cell glycolysis mainly through targeting the miR-1179/SPAG5 [23]. LncRNA FAM83A-AS1 contributed to cell proliferation and stemness via the HIF-1α/glycolysis axis [24]. Cao et al. identified four critical glycolysis-related LncRNAs associated with prognosis [25]. Therefore, searching for new LncRNAs in LUAD targeting glycolysis is of great significance.

LINC00908 is a recently identified lncRNA. Wang et al. demonstrated that LINC00908 was downregulated, associated with poor OS in TNBC and encoded a polypeptide, ASRPS [26]. Shan et al. showed that LINC00908 was significantly upregulated, promoted proliferation and inhibited apoptosis of colorectal cancer cells by regulating KLF5 expression [27]. However, the clinical values and detail roles of LINC00908 in LUAD progression remain largely unknown. Our data suggest multiple functions of LINC00908 that contribute to tumorigenesis in LUAD. In this study, we first delineated the critical role of LINC00908 in regulating LUAD growth and progression. More importantly, LINC00908 suppresses LUAD cell aerobic glycolysis through inhibition of DDX54 expression.

Studies suggested that several DDX family members regulating mRNA translation in cancer cells. DDX inhibitors have been under development. DDX54, a member of the DDX family, was reported to be play a

cancerous role in colorectal cancer [28]. Our data suggest that high DDX54 expression predicts poorer PFS and OS in LUAD patients. In addition, knockdown of DDX54 abolished the ability of LINC00908 to regulate LUAD cell proliferation, migration, invasion, and glycolysis. The molecular and functional interaction between DDX54 and LINC00908 described in our report represents a critical mechanism in LUAD.

Recent studies have shown that dysregulation of LncRNA is associated with oncogenic transcription factors [29]. Investigations of the function of regulatory factor X (RFX) have shown that RFX regulates genes involved in various cellular and developmental processes. Dysregulation of RFX is highly associated with severe disease states [30]. RFX2 were identified as one of the master transcription factors in regulating angiogenesis signature in kidney renal clear cell carcinoma patients [31]. In our study, RFX2 was confirmed to regulate the expression of LINC00908, and 2 predicted binding sites for RFX2 in the LINC00908 promoter were proved. Here we explored a mechanism of RFX2 in controlling LUAD cell growth and inhibiting glycolysis through upregulation of LINC00908 expression. Based on these findings, we speculate that RFX2/LINC00908/DDX54 axis has critical biological functions in LUAD.

In conclusion, our study reveals a distinctive mechanism regulating LINC00908 in LUAD. RFX2/LINC00908/DDX54 axis regulates LUAD cell proliferation, migration, invasion and glycolysis in vitro and in vivo, which is a potential therapeutic target for the prevention and treatment of LUAD.

Declarations

ACKNOWLEDGMENTS

This work was supported by the Capacity Building Continuing Education Center Foundation from National Health Commission of China (GWJJ2021100304).

DATA AVAILABILITY

The data used to support the findings of this study are included within the article.

AUTHOR CONTRIBUTIONS

X.Y., X.Z., and Y.H. designed the study. X.Y. and X.Z. analyzed the data, and wrote the manuscript. Y.H. and X.Z. supervised the project. X.Y., J.Z., Y.Z. and L.Z. performed experiments. L.W., X.H., H.T., and F.Z. helped to collect the tissue samples. C.L., X.Z. conducted animal experiments. All authors read and approved the final manuscript.

DECLARATION OF INTERESTS

The authors declare no competing interests.

References

1. Siegel RL, Miller KD, Fuchs HE, Jemal A. Cancer statistics, 2022. CA Cancer J Clin 2022, 72(1): 7–33.
2. Wu F, Wang L, Zhou C. Lung cancer in China: current and prospect. Curr Opin Oncol 2021, 33(1): 40–46.
3. Succony L, Rassl DM, Barker AP, McCaughan FM, Rintoul RC. Adenocarcinoma spectrum lesions of the lung: Detection, pathology and treatment strategies. Cancer Treat Rev 2021, 99: 102237.
4. Hanahan D. Hallmarks of Cancer: New Dimensions. Cancer Discov 2022, 12(1): 31–46.
5. Faubert B, Li KY, Cai L, Hensley CT, Kim J, Zacharias LG, *et al.* Lactate Metabolism in Human Lung Tumors. Cell 2017, 171(2): 358–371 e359.
6. Li L, Liang Y, Kang L, Liu Y, Gao S, Chen S, *et al.* Transcriptional Regulation of the Warburg Effect in Cancer by SIX1. Cancer Cell 2018, 33(3): 368–385 e367.
7. Hu Y, Mu H, Deng Z. The transcription factor TEAD4 enhances lung adenocarcinoma progression through enhancing PKM2 mediated glycolysis. Cell Biol Int 2021, 45(10): 2063–2073.
8. Kopp F, Mendell JT. Functional Classification and Experimental Dissection of Long Noncoding RNAs. Cell 2018, 172(3): 393–407.
9. Peng WX, Koirala P, Mo YY. LncRNA-mediated regulation of cell signaling in cancer. Oncogene 2017, 36(41): 5661–5667.
10. Jia M, Li Z, Pan M, Tao M, Wang J, Lu X. LINC-PINT Suppresses the Aggressiveness of Thyroid Cancer by Downregulating miR-767-5p to Induce TET2 Expression. Mol Ther Nucleic Acids 2020, 22: 319–328.
11. Xu X, Chen X, Shen X, Chen R, Zhu C, Zhang Z, *et al.* Genome-wide identification and characterization of DEAD-box helicase family associated with early somatic embryogenesis in Dimocarpus longan Lour. J Plant Physiol 2021, 258–259: 153364.
12. Yang P, Li J, Peng C, Tan Y, Chen R, Peng W, *et al.* TCONS_00012883 promotes proliferation and metastasis via DDX3/YY1/MMP1/PI3K-AKT axis in colorectal cancer. Clin Transl Med 2020, 10(6): e211.
13. Karmakar S, Rauth S, Nallasamy P, Perumal N, Nimmakayala RK, Leon F, *et al.* RNA Polymerase II-Associated Factor 1 Regulates Stem Cell Features of Pancreatic Cancer Cells, Independently of the PAF1 Complex, via Interactions With PHF5A and DDX3. Gastroenterology 2020, 159(5): 1898–1915 e1896.
14. Zhang M, Weng W, Zhang Q, Wu Y, Ni S, Tan C, *et al.* The lncRNA NEAT1 activates Wnt/beta-catenin signaling and promotes colorectal cancer progression via interacting with DDX5. J Hematol Oncol 2018, 11(1): 113.
15. Paine I, Posey JE, Grochowski CM, Jhangiani SN, Rosenheck S, Kleyner R, *et al.* Paralog Studies Augment Gene Discovery: DDX and DHX Genes. Am J Hum Genet 2019, 105(2): 302–316.
16. Milek M, Imami K, Mukherjee N, Bortoli F, Zinnall U, Hazapis O, *et al.* DDX54 regulates transcriptome dynamics during DNA damage response. Genome Res 2017, 27(8): 1344–1359.

17. Zhang Y, Guo H, Zhang H. SNHG10/DDX54/PBX3 Feedback Loop Contributes to Gastric Cancer Cell Growth. Dig Dis Sci 2021, 66(6): 1875–1884.
18. Xie Y, Wang M, Xia M, Guo Y, Zu X, Zhong J. Ubiquitination regulation of aerobic glycolysis in cancer. Life Sci 2022, 292: 120322.
19. Abbaszadeh Z, Cesmeli S, Biray Avci C. Crucial players in glycolysis: Cancer progress. Gene 2020, 726: 144158.
20. Abdel-Wahab AF, Mahmoud W, Al-Harizy RM. Targeting glucose metabolism to suppress cancer progression: prospective of anti-glycolytic cancer therapy. Pharmacol Res 2019, 150: 104511.
21. Lin W, Zhou Q, Wang CQ, Zhu L, Bi C, Zhang S, *et al.* LncRNAs regulate metabolism in cancer. Int J Biol Sci 2020, 16(7): 1194–1206.
22. Bhan A, Soleimani M, Mandal SS. Long Noncoding RNA and Cancer: A New Paradigm. Cancer Res 2017, 77(15): 3965–3981.
23. Wang L, Cao L, Wen C, Li J, Yu G, Liu C. LncRNA LINC00857 regulates lung adenocarcinoma progression, apoptosis and glycolysis by targeting miR-1179/SPAG5 axis. Hum Cell 2020, 33(1): 195–204.
24. Chen Z, Hu Z, Sui Q, Huang Y, Zhao M, Li M, *et al.* LncRNA FAM83A-AS1 facilitates tumor proliferation and the migration via the HIF-1alpha/ glycolysis axis in lung adenocarcinoma. Int J Biol Sci 2022, 18(2): 522–535.
25. Cao P, Zhao B, Xiao Y, Hu S, Kong K, Han P, *et al.* Understanding the Critical Role of Glycolysis-Related lncRNAs in Lung Adenocarcinoma Based on Three Molecular Subtypes. Biomed Res Int 2022, 2022: 7587398.
26. Wang Y, Wu S, Zhu X, Zhang L, Deng J, Li F, *et al.* LncRNA-encoded polypeptide ASRPS inhibits triple-negative breast cancer angiogenesis. J Exp Med 2020, 217(3).
27. Shan TD, Tian ZB, Li Q, Jiang YP, Liu FG, Sun XG, *et al.* Long intergenic noncoding RNA 00908 promotes proliferation and inhibits apoptosis of colorectal cancer cells by regulating KLF5 expression. J Cell Physiol 2021, 236(2): 889–899.
28. Yu Y, Wang JL, Meng LL, Hu CT, Yan ZW, He ZP, *et al.* DDX54 Plays a Cancerous Role Through Activating P65 and AKT Signaling Pathway in Colorectal Cancer. Front Oncol 2021, 11: 650360.
29. Long Y, Wang X, Youmans DT, Cech TR. How do lncRNAs regulate transcription? Sci Adv 2017, 3(9): eaao2110.
30. Sugiaman-Trapman D, Vitezic M, Jouhilahti EM, Mathelier A, Lauter G, Misra S, *et al.* Characterization of the human RFX transcription factor family by regulatory and target gene analysis. BMC Genomics 2018, 19(1): 181.
31. Zheng W, Zhang S, Guo H, Chen X, Huang Z, Jiang S, *et al.* Multi-omics analysis of tumor angiogenesis characteristics and potential epigenetic regulation mechanisms in renal clear cell carcinoma. Cell Commun Signal 2021, 19(1): 39.

Figures

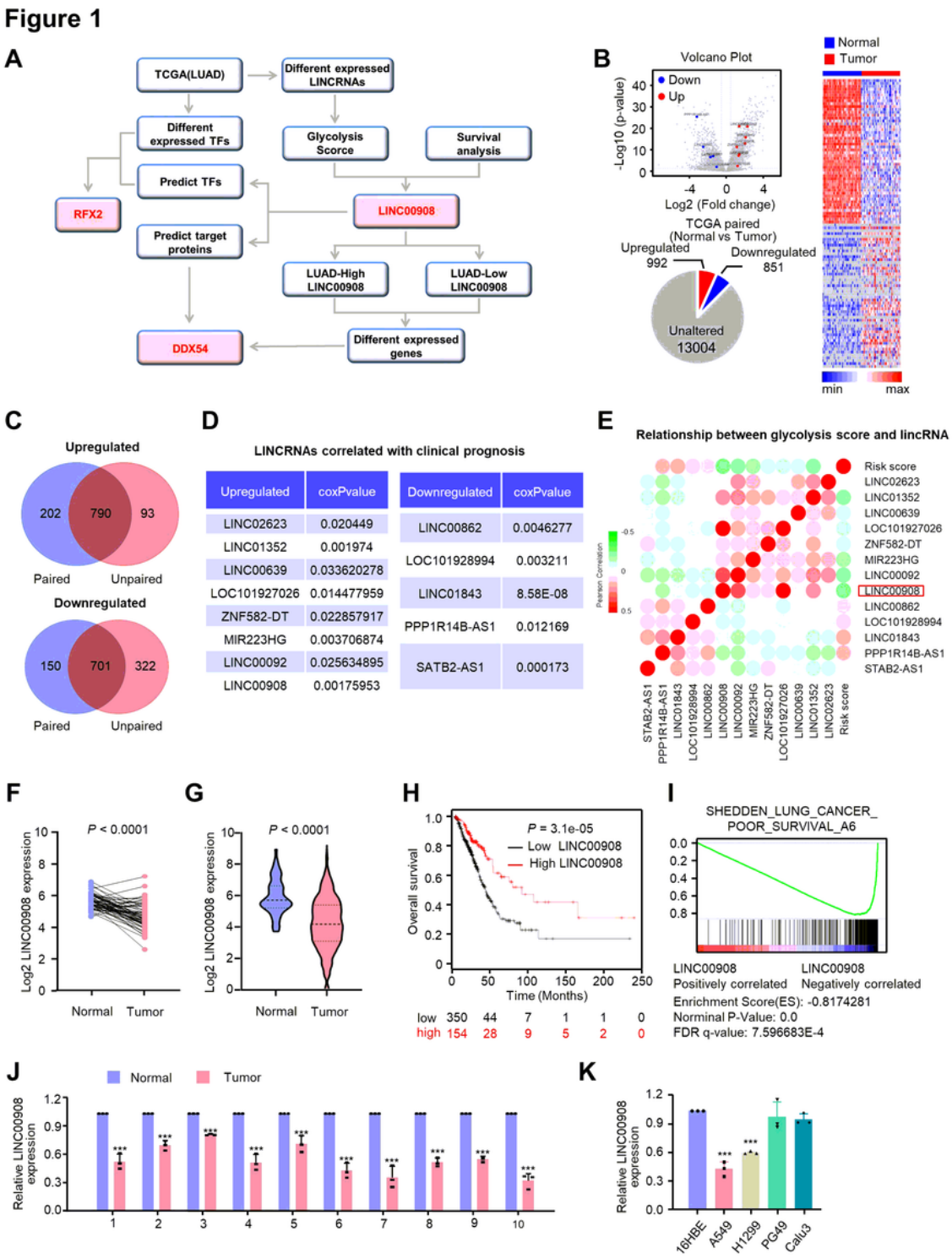

Figure 1

Screening of LncRNAs and characterization of LINC00908 in LUAD. (**A**) Screening flowchart. (**B**) A volcano plot illustrating differential LncRNA expressions between paired normal and tumor LUAD tissues based on TCGA database. Values are presented as the log10 of tag counts. (**C**) Venn analysis of the

differentially regulated LncRNAs. The middle portion were the intersection of differentially regulated LncRNAs in paired and unpaired LUAD tissues. (**D**) Screened LncRNAs in the TCGA clinical database by independent prognostic analysis. (**E**) Correlations between clinical prognosis related LncRNAs and the risk score related to glycolysis. (**F, G**) LINC00908 expressions in TCGA LUAD database. (**H**) Kaplan–Meier estimate of overall survival related to LINC00908 expressions in LUAD patients. (**I**) GSEA plot for LINC00908 expression in the TCGA LUAD dataset. (**J**) RT-PCR analysis of LINC00908 expressions in 10 paired adjacent and tumor tissues. (**K**) Expression of LINC00908 in one human bronchial epithelioid cell and four LUAD cell lines by RT-PCR. ***$P < 0.0001$.

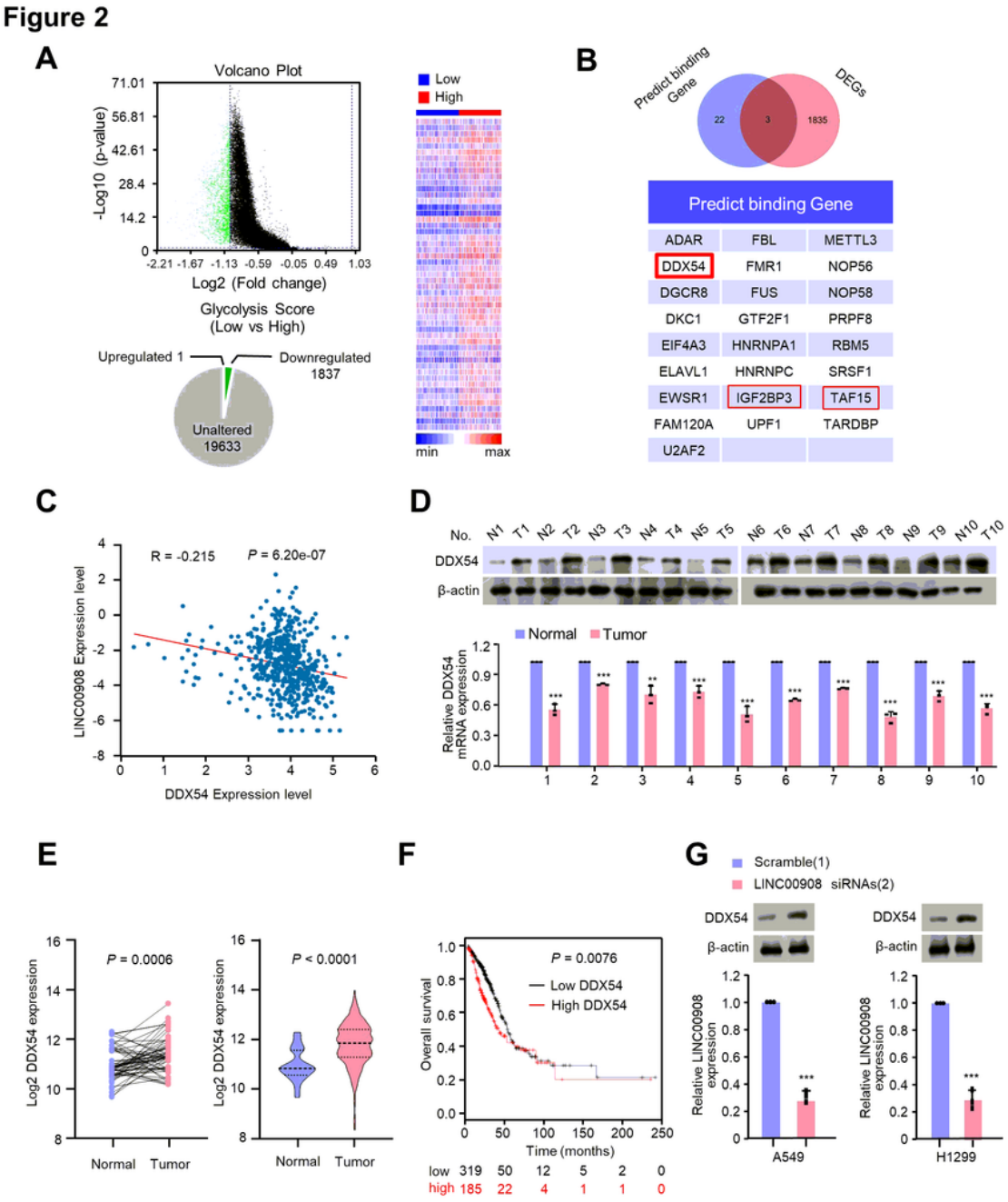

Figure 2

DDX54, a negative prognostic factor for LUAD, is regulated by LINC00908. (**A**) Volcano plot illustrating DEGs from RNA-seq analysis between high and low risk score. Values are presented as the log10 of tag counts. Pie chart showed screened genes. The hierarchical clustering of the RNA-seq analysis for differently expressed genes. (**B**) Venn diagram of target genes of LINC00908(bottom table) by https://starbase.sysu.edu.cn (left) or DEGs (right). (**C**) The relationship between the expression of

LINC00908 and DDX54 in LUAD based on TCGA database by online analysis (https://starbase.sysu.edu.cn). (**D**) DDX54 expressions in 10 paired tumor and adjacent normal tissues. (**E**) DDX54 expression in tumor and adjacent normal tissues in TCGA database. (**F**) Kaplan–Meier estimate of OS for LUAD patients from TCGA (http://kmplot.com/analysis/). (**G**) The DDX54 protein levels of and LINC00908 mRNA levels in LUAD cell lines. ***P< 0.0001.

Figure 3

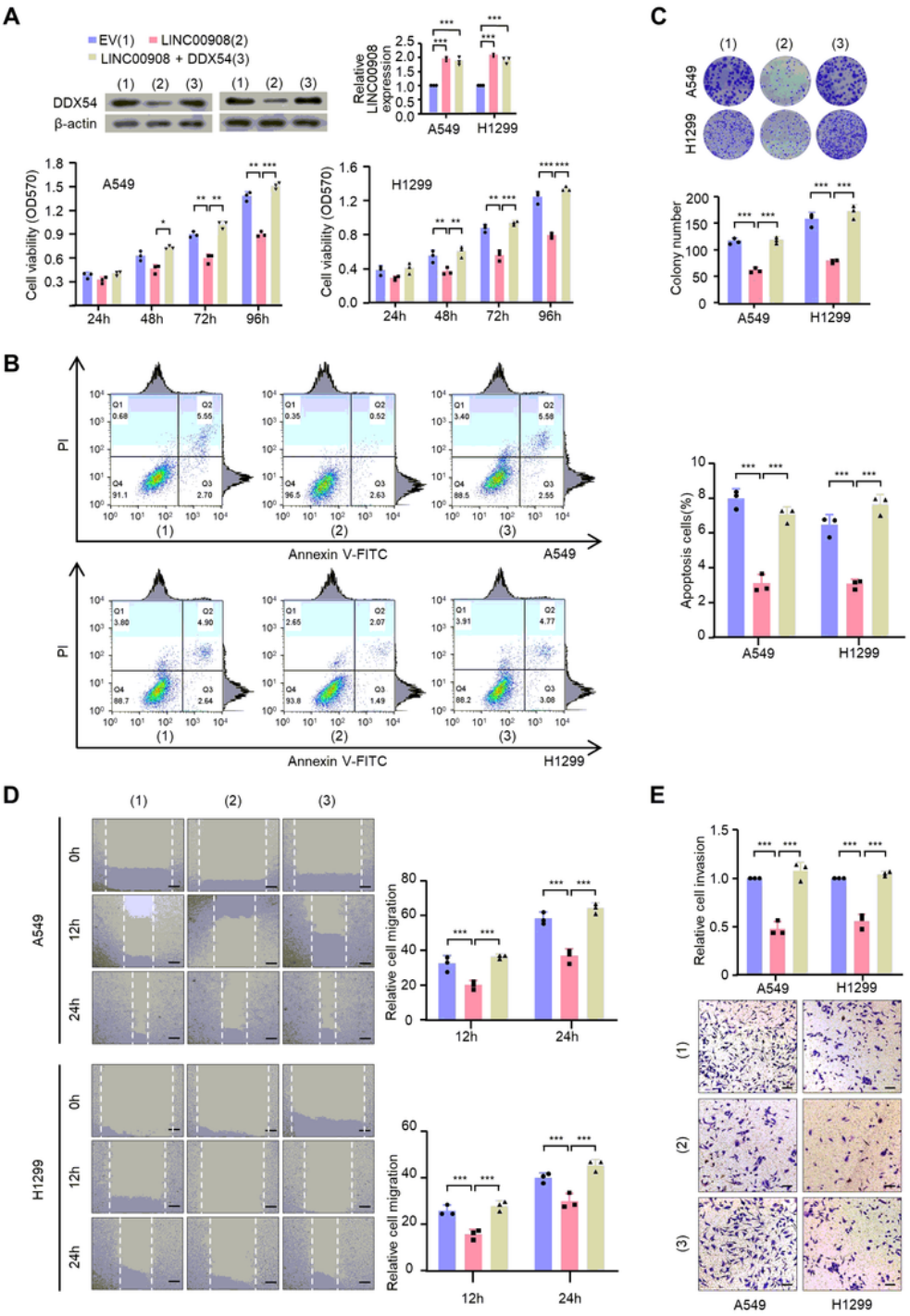

Figure 3

LINC00908 inhibition facilitated LUAD tumorigenesis through mediating DDX54 in vitro. (**A**) LUAD cells were transfected with empty vector (1) or LINC00908 (2) or LINC00908 plus DDX54 (3). The representative immunoblot shows DDX54 expression. LINC00908 expression were determined by qRT-PCR. Histograms showed the proliferation of indicated cells. (**B**) Cell apoptosis in both cells were evaluated by flow cytometry. (**C**) Cell growth of LINC00908 or LINC00908 plus DDX54 or control in both cells were tested by colony formation assays. (**D**) Cell migration of LINC00908 or LINC00908 plus DDX54 in both cells were tested by wound-healing assays. (**E**) Transwell assays of invasion in LINC00908 or LINC00908 plus DDX54 or control in both cells. *$P < 0.05$, **$P < 0.001$, ***$P < 0.0001$.

Figure 4

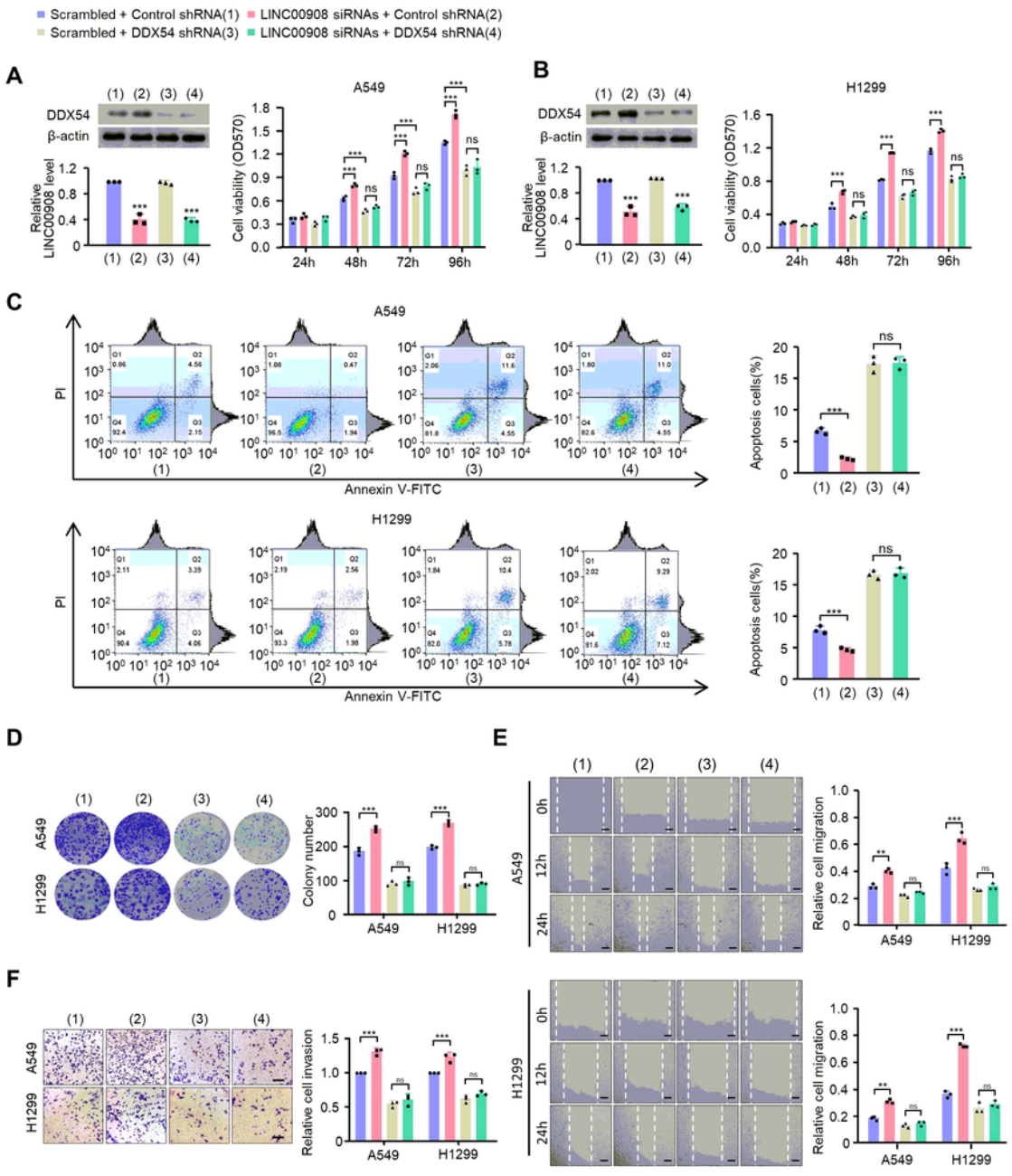

Figure 4

DDX54 knockdown reversed the downregulation of LINC00908 in LUAD in vitro. (**A, B**) A549 and H1299 cells proliferation transfected with scramble plus control shRNA (1) or LINC00908 siRNAs plus control shRNA (2) or scramble plus DDX54 shRNA (3) or LINC00908 siRNAs plus DDX54 shRNA (4). (**C**) Cell apoptosis in two cell lines were evaluated by flow cytometry, and the apoptotic cell percentage was statistically analyzed. (**D-F**) Illustrative images show colonies in plates, cell migration and invasion.

Histograms show colony number, comparative cell migration and invasion. *P < 0.05, **P< 0.001, ***P < 0.0001.

Figure 5

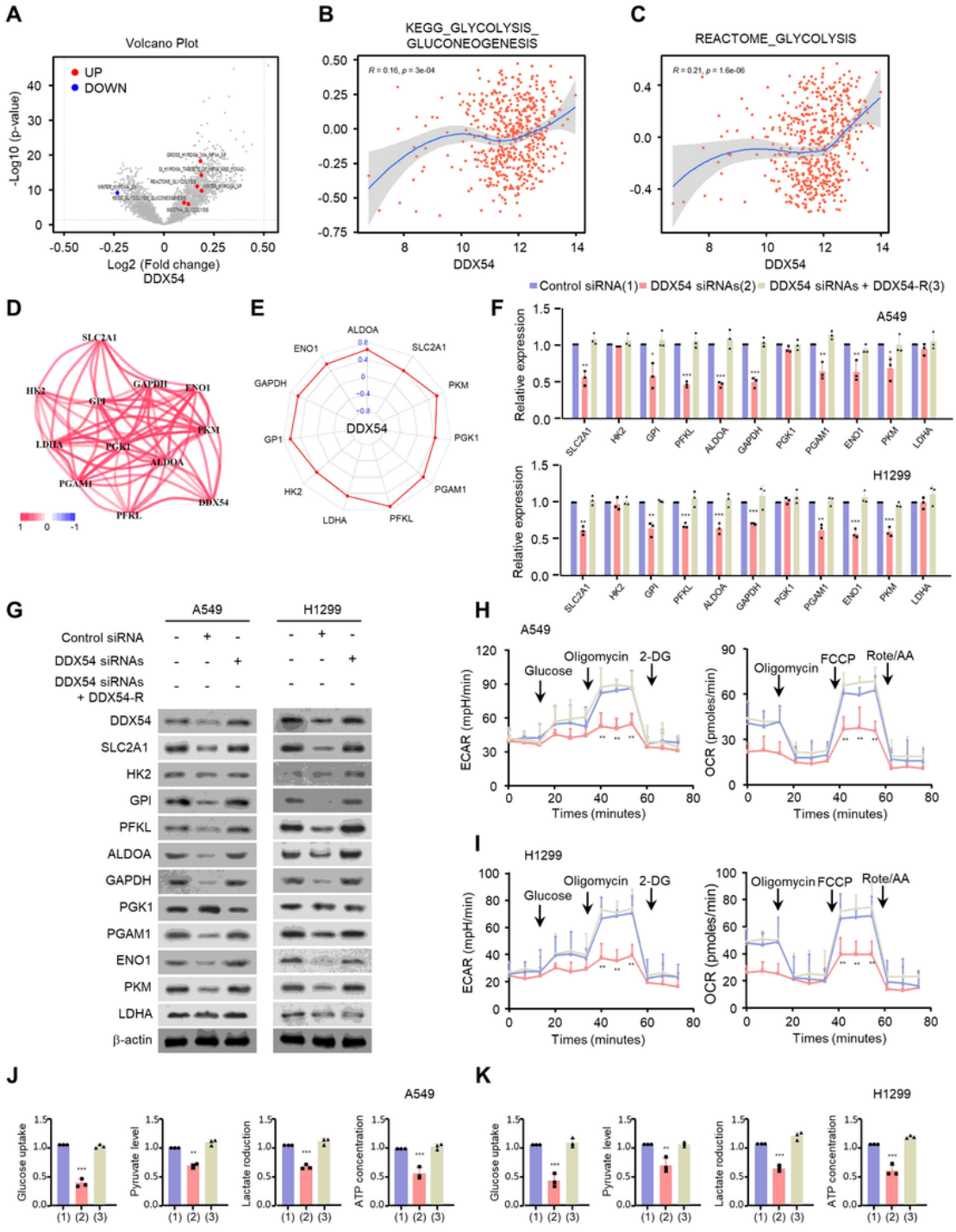

Figure 5

DDX54 knockdown downregulates glycolysis in LUAD cells. (**A**) GSVA analysis showed 1 downregulated and 6 upregulated glycolysis related pathways between high and low DDX54 group. (**B**) The relationship

between DDX54 expression and KEGG_GLYCOLYSIS_GLUCONEOGENESIS. (**C**) The relationship between DDX54 expression and REACTOME_GLYCOLYSIS. (**D, E**) The correlation coefficient between DDX54 expression level and 11 glycolysis-related genes. (**F, G**) The mRNA and protein levels of 11 glycolysis-related genes in A549 and H1299 cells transfected with control siRNA (1) or DDX54 siRNAs (2) or DDX54 siRNAs plus DDX54-R (3). (**H-K**) A549 and H1299 cells were transfected as in (F). ECAR, OCR, Glucose uptake, Pyruvate, Lactate production and ATP production were measured. *P < 0.05, **P< 0.001, ***P < 0.0001.

Figure 6

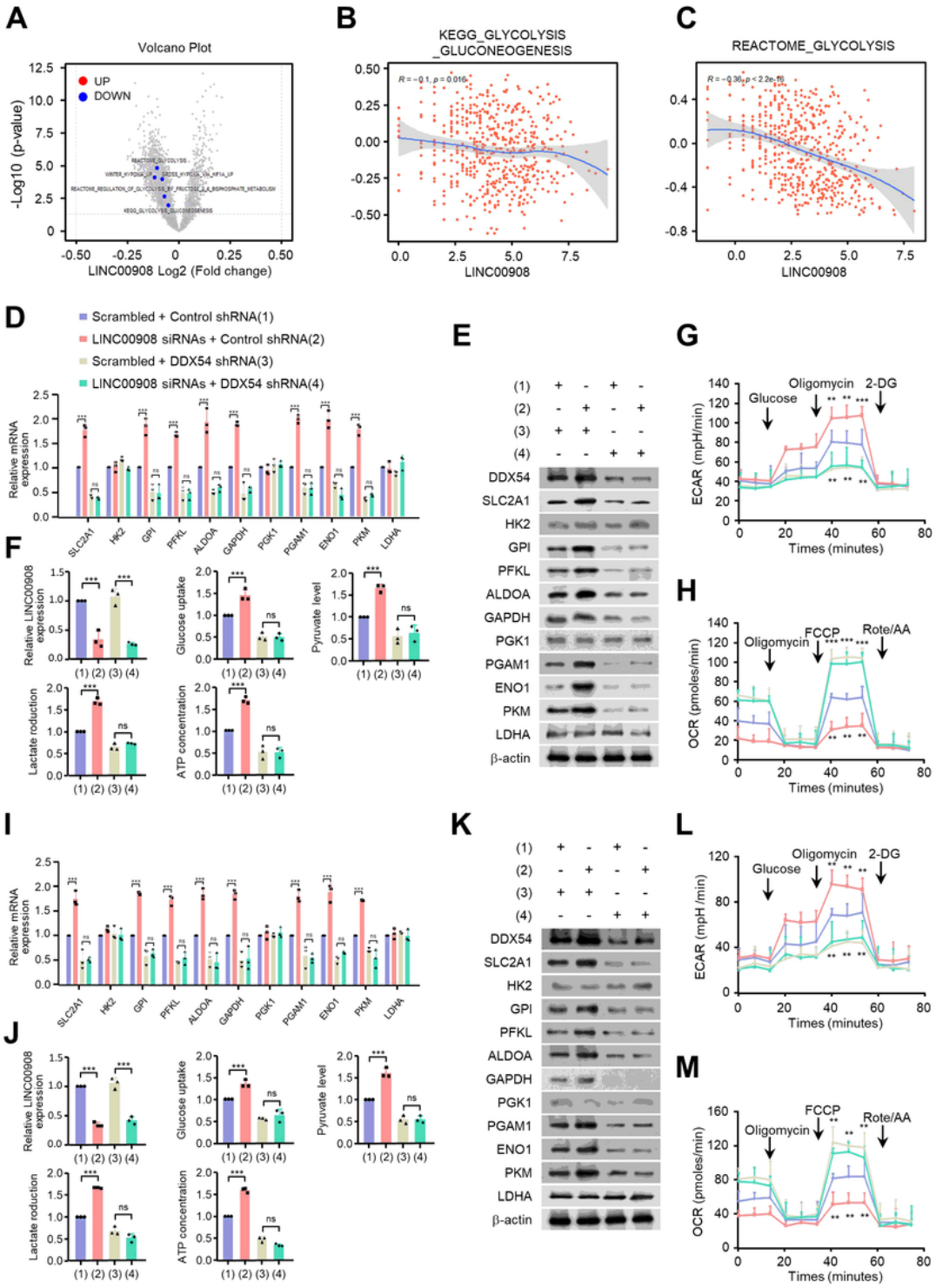

Figure 6

LINC00908 downregulates glycolysis through DDX54 in vitro. (**A**) There are 5 downregulated glycolysis related pathways between high and low LINC00908 groups by GSVA analysis. (**B**) The relationship between LINC00908 expression and KEGG_GLYCOLYSIS_GLUCONEOGENESIS. (**C**) The relationship between DDX54 expression and REACTOME_GLYCOLYSIS. (**D, E**) The mRNA and protein levels of 11 glycolysis-related genes in A549 and H1299 cells transfected with scramble plus control shRNA (1) or LINC00908 siRNAs plus control shRNA (2) or scramble plus DDX54 siRNAs (3) or LINC00908 siRNAs plus DDX54 siRNAs (4). (**F-M**) A549 and H1299 cells were transfected as in (D). ECAR, OCR, Glucose uptake, Pyruvate, Lactate production and ATP production were measured. *$P < 0.05$, **$P < 0.001$, ***$P < 0.0001$.

Figure 7

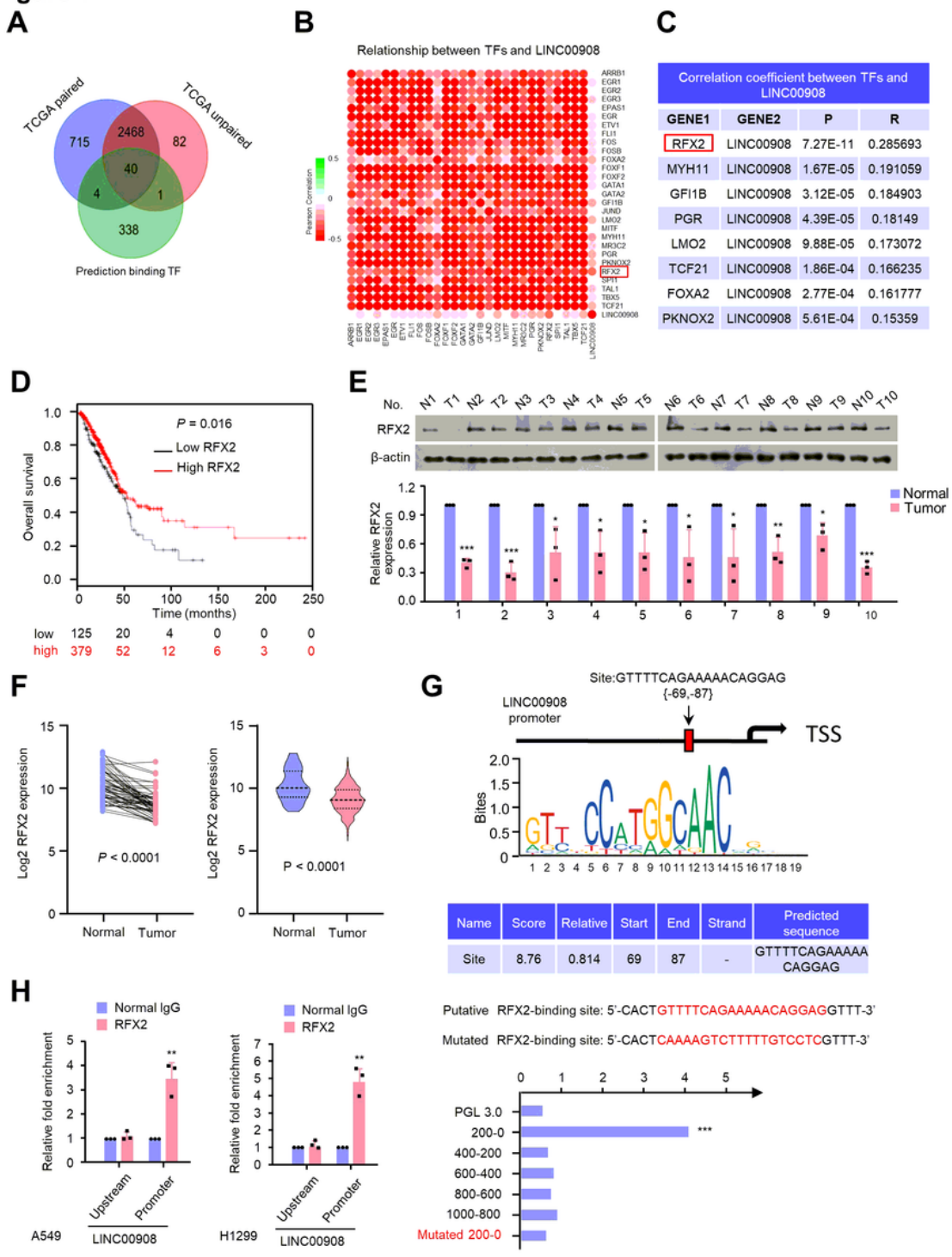

Figure 7

RFX2 was screened as one of the transcript factors of LINC00908. (**A**) Venn analysis of the DEGs and predicted TFs. The mediumpurple and red circles represent the DEGs in paired and unpaired LUAD tissues. The green circle represents the predicted TFs targeting LINC00908 by online analysis (https://jaspar.genereg.net/). The intersection of the results were 40 TFs. (**B**) The correlation matrix between LINC00908 expression and 28 positive prognosis transcript factors in LUAD. (**C**) The correlation

coefficient between LINC00908 expression and the most relevant 8 transcription factors using pearson analysis. (**D**) Kaplan–Meier estimate of OS for RFX2 in LUAD patients from TCGA (http://kmplot.com/analysis/). (**E**) RFX2 expression in 10 paired tumor and adjacent normal tissues were detected using real-time RT-PCR and Western-blot. (**F**) RFX2 expression between tumor and adjacent normal tissues in TCGA database were displayed. (**G**) A conserved RFX2-binding element at the LINC00908 promoter was predicted by JASPAR (http:/jaspar.genereg.net). Luciferase activity of different LINC00908 promoter reporters in A549 cells. (**H**) CHIP analysis of RFX2 occupancy on the LINC00908 promoter or upstream in A549 and H1299 cells. *$P < 0.05$, **$P < 0.001$, ***$P < 0.0001$.

Figure 8

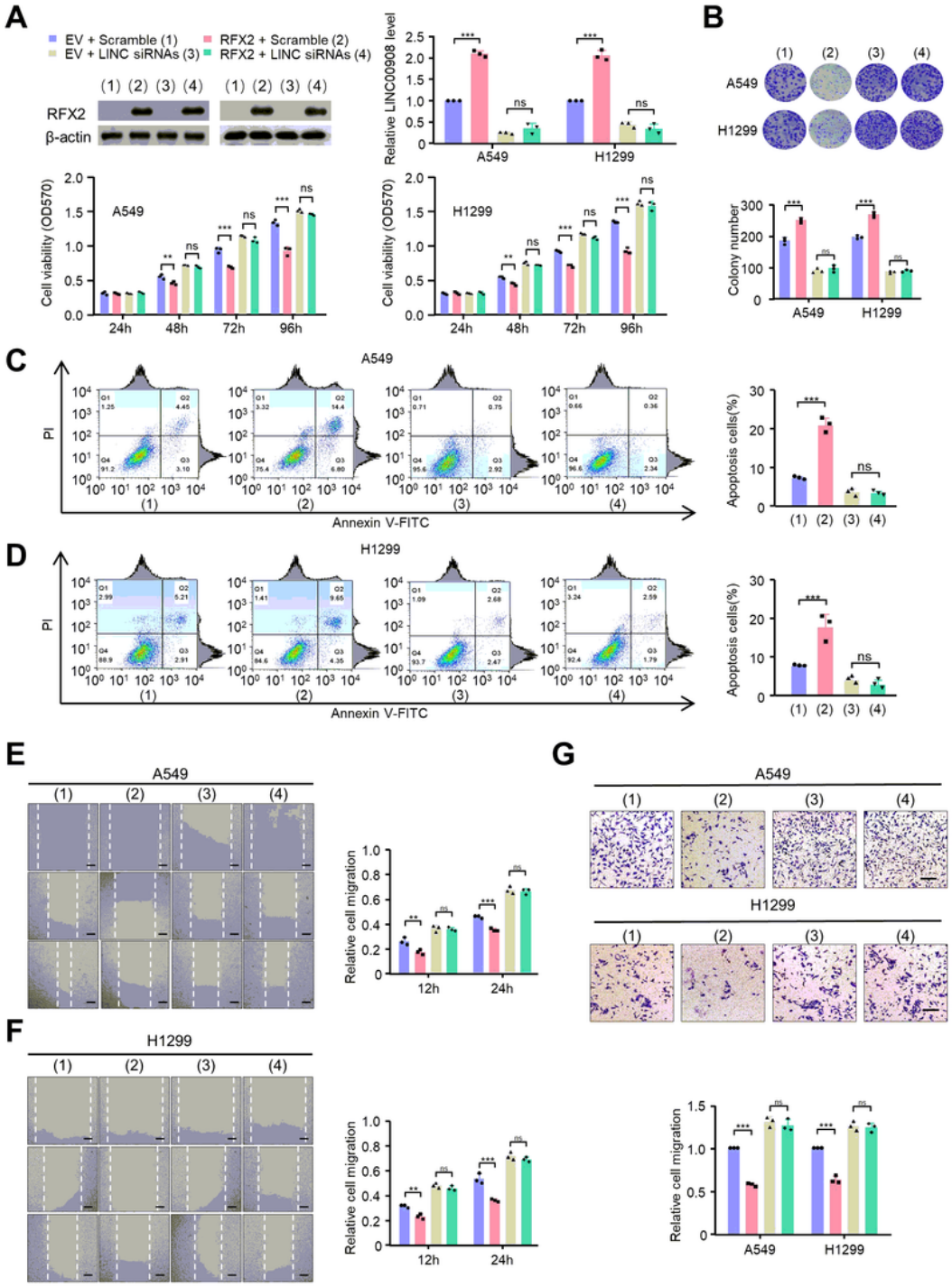

Figure 8

RFX2 suppresses proliferation, apoptosis, migration, invasion and glycolysis by regulating LINC00908 in LUAD cells. A549 and H1299 cells were transfected with empty vector plus scramble (1) or RFX2 plus scramble (2) or empty vector plus LINC00908 siRNAs (3) or RFX2 plus LINC00908 siRNAs (4). (**A**) The immunoblot shows RFX2 in the 4 above-mentioned groups. LINC00908 knockdown lead to RFX2 inactivation in regulating cell proliferation. Illustrative images show colonies in plates (**B**), cell migration

(**C**) and invasion (**D**). Histograms show proliferation, colony number, comparative cell migration and invasion. *P< 0.05, **P < 0.001, ***P < 0.0001.

Figure 9

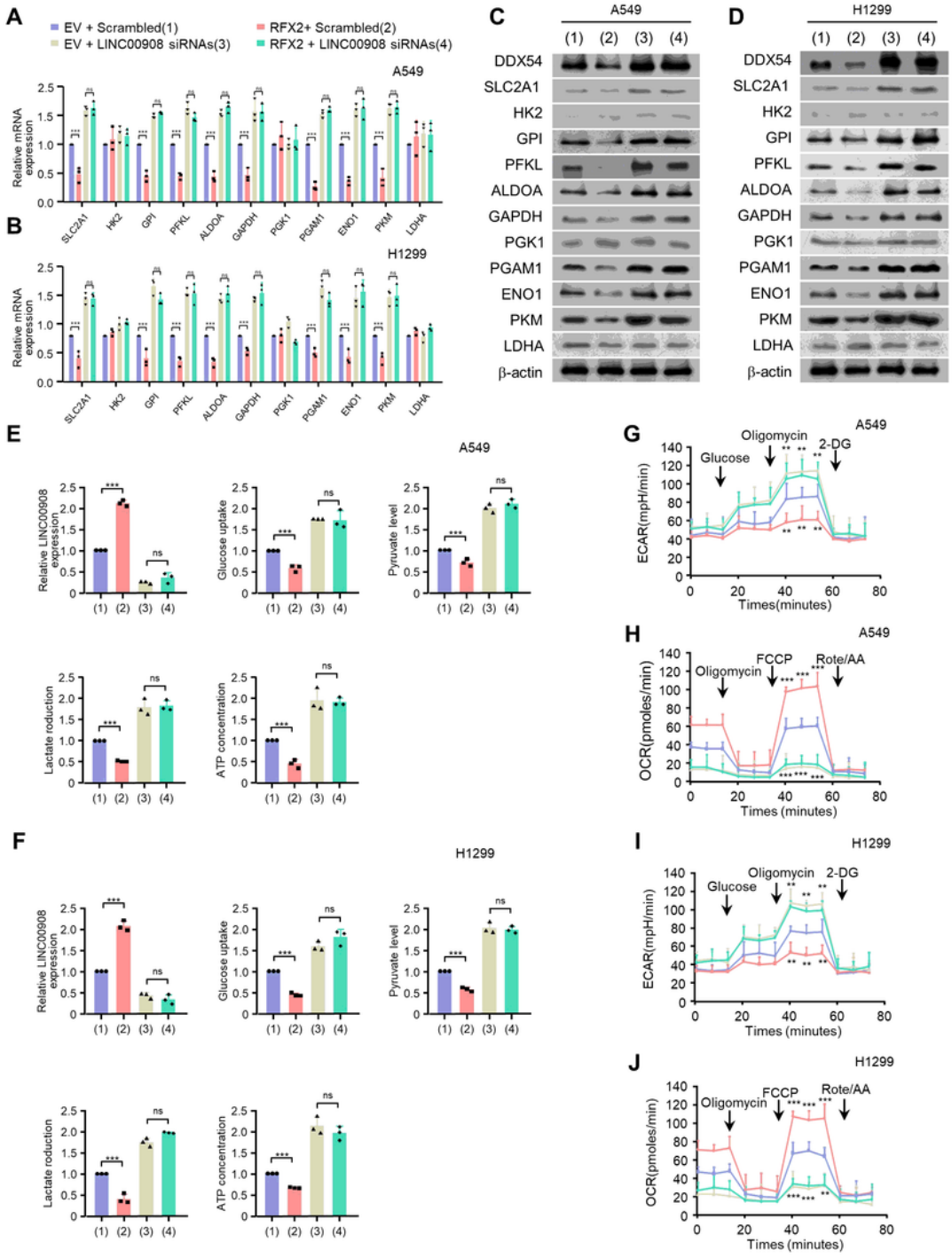

Figure 9

RFX2 downregulates glycolysis through LINC00908 in vitro. A549 and H1299 cells were transfected with empty vector plus scramble (1) or RFX2 plus scramble (2) or empty vector plus LINC00908 siRNAs (3) or

RFX2 plus LINC00908 siRNAs (4). (**A-D**) The mRNA and protein levels of 11 glycolysis-related genes were measured. (**E-J**) ECAR, OCR, Glucose uptake, Pyruvate, Lactate production and ATP production were detected. *$P < 0.05$, **$P < 0.001$, ***$P < 0.0001$.

Figure 10

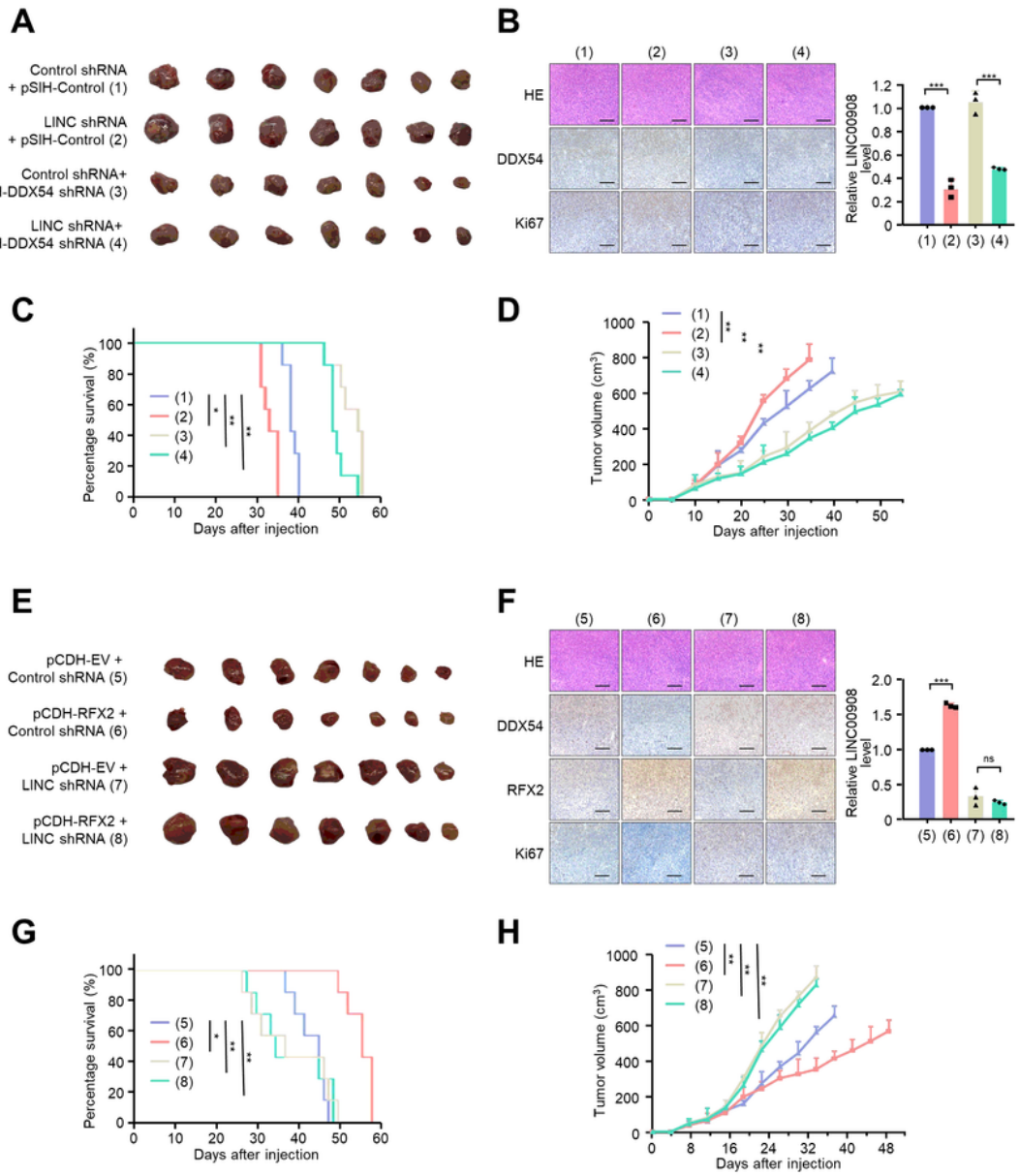

Figure 10

RFX2/LINC00908/DDX54 axis has a tumor-promoting effect in vivo. (**A, E**) Representative images of tumors from the mice subcutaneously inoculated with A549 cells expressing the indicated constructs. (**B, F**) Representative HE staining. (**C, D, G, H**) Survival and growth curve were measured and plotted. All data were presented as the mean ± s.e.m. (n = 7 per group).

Figure 6

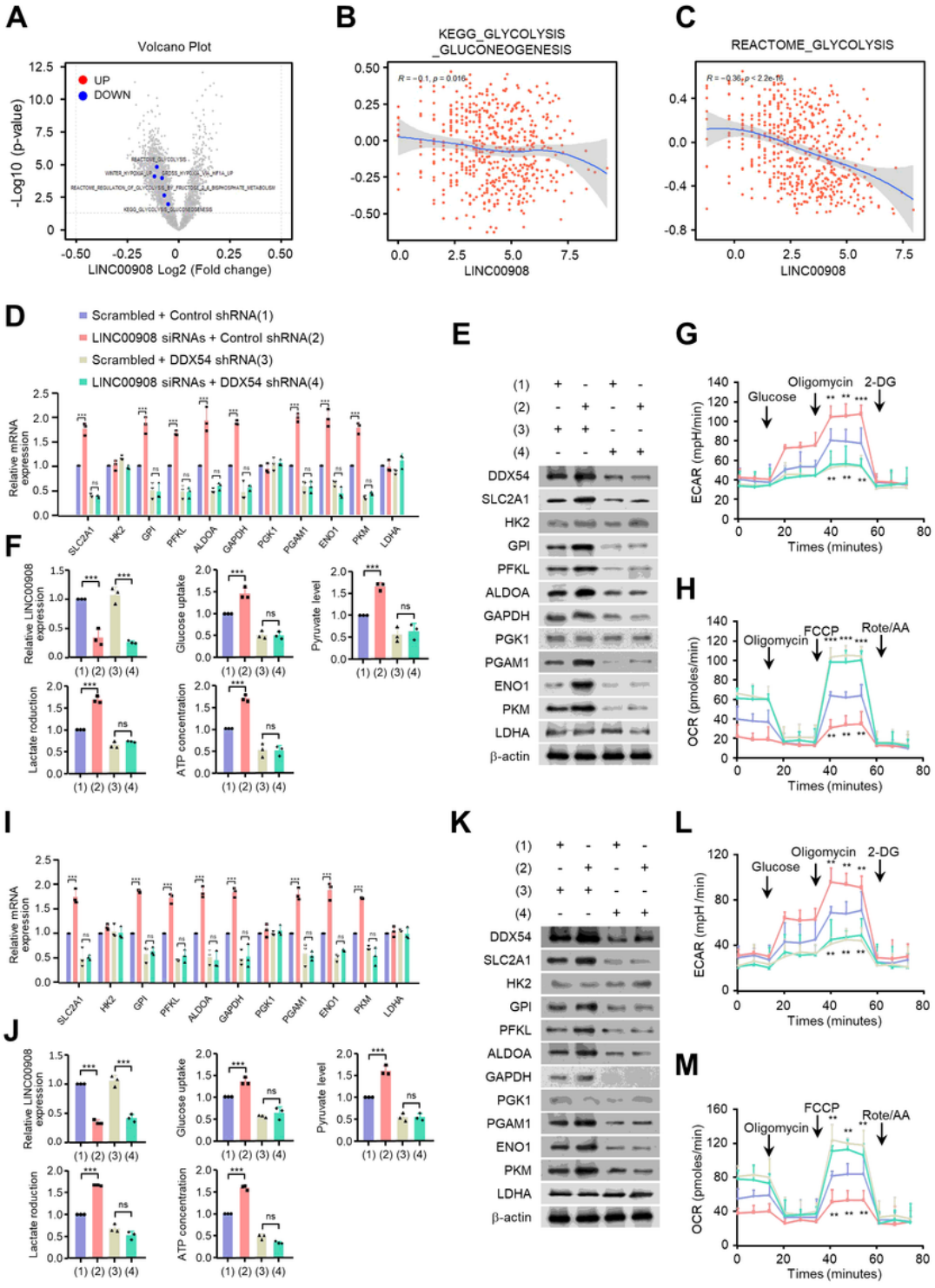

Figure 11

Clinical Relevance of LINC00908, DDX54 and RFX2 in the LUAD patients. (**A**) Representative FISH staining for LINC00908 and IHC staining for RFX2, DDX54, ki67 in LUAD patients. (**B**) Correlation between LINC00908 DDX54 and RFX2 expressions of the specimens percentage. (**C**) Schematic of the regulatory network of LUAD in this study.

Supplementary Files

This is a list of supplementary files associated with this preprint. Click to download.

- FigureS1.tif
- FigureS2.tif
- FigureS3.tif
- FigureS4.tif
- DiffLncRNAs.xlsx
- Diffgene.xlsx
- Diffpathway.xlsx
- GlycolysisrelatedLncRNAs.xlsx
- PredictbindingTFs.xlsx
- Predictbindinggenes.xlsx